# Optimum Wavelength Selection to Extend the Unambiguous Measurement Range of the Three-Wavelength Single-Shot Interferometry

**Katsuichi KITAGAWA***

This paper presents a novel method for selecting optimum measurement wavelengths in multi-wavelength interferometry. It is based on a coincidence error analysis in exact fractions solutions. By this method, three wavelengths of 470, 560, and 600 nm have been selected. With these wavelengths, a surface profiler has been developed using three-wavelength single-shot interferometry, and an extended measurement range over 8 μm has been experimentally proved.

**Key Words**. Interferometry, Surface profiler, Three-wavelength, Single-shot, Optimum wavelength

## 1. Introduction

The surface shape measurement method based on optical interference is widely used in industry as an ultra-high-precision three-dimensional measurement method, but there is a problem that the accuracy is greatly reduced in an environment with disturbance such as vibration. As a solution to this problem, a one-shot interferometry method, which is called spatial carrier fringe method [1)-7)], which introduces carrier fringes by inclining the reference plane and obtains a three-dimensional shape from one fringe image, has been proposed (Fig. 1). From one interference fringe image (Fig. 2) obtained by this method, the surface shape is obtained by the Fourier transform method [2)], the spatial phase synchronization method [3)-5)], the local model fitting method [6) 7)], etc.

However, the spatial carrier fringe method, like the phase shift method, requires phase unwrapping to obtain the height from the obtained phase. Since the phase period ($2\pi$) corresponds to 1/2 of the light source wavelength, the phases are connected on the assumption that the step between adjacent pixels is 1/4 or less of the light source wavelength. Due to this step limit, it cannot be applied to measurement objects with large steps. In order to solve this problem, the author have proposed a multi-wavelength single-shot measurement method and succeeded in measuring a 350 nm step height [8)9)] by two wavelengths and a 1μm step height by three wavelengths [10) 11)].

By the way, in these reports, since the commercially available RGB-LED lighting was used, the three wavelengths were fixed at B: 470 nm, G: 530 nm, and R: 627 nm. However, in order to further expand the measurement range of the three-wavelength single-shot method, it is expected that there will be an optimal combination of wavelengths used.

Expanding the measurement range by using multiple wavelengths is common to the multi-wavelength phase shifting method [12)] and the multi-wavelength interferometry [13)] used for calibration of gauge blocks. However, most of the multi-wavelength methods reported so far use a laser light source, so the wavelength is limited, and there are few reports on wavelength optimization.

Pförtner et al.[14)] used three lasers, and say it is desirable that the wavelengths are relatively prime and have no common divisor. Towers et al.[15)] proposed a method of determining the three wavelengths so that the equivalent wavelengths are in the geometric series, but do not describe the specific wavelengths. Falaggis et al. [16)] proposed an optimal wavelength search method based on the coincidence method for multi-wavelength interferometry using the near-infrared band. However, it only describes the condition that should be avoided and cannot be said to be a general optimization

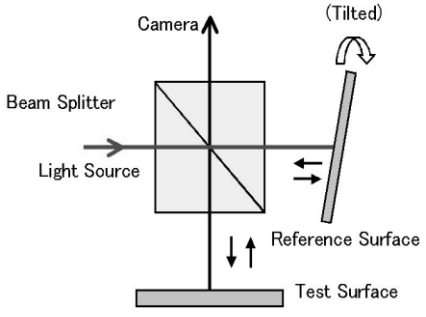


**Fig. 1** Optics of spatial carrier interferometry

**Fig. 2** Interferogram with carrier fringes

* R&D Div., Toray Engineering Co., Ltd., 1–1–45 Oe, Otsu
（Received May 13, 2013）
（Revised October 25, 2013）

method. As mentioned above, no clear solution to this problem has been reported.†1

In this paper, the outline of three-wavelength single-shot interferometry is given in Chapter 2, the coincidence algorithm and the estimation method of the measurement range are reported in Chapter 3, and the searched optimum wavelength combination and the experimental results using the three wavelengths are reported in Chapter 4.†2

## 2. Three-wavelength single-shot interferometry

In this chapter, we outline the three-wavelength single-shot interferometry proposed by the authors. [10)11)]

### 2.1 Interferometric optics and imaging system

As shown in Fig. 1, in the two-beam interference system, the reference plane is inclined and carrier fringes are introduced. The 3-wavelength imaging system consists of a commercially available 3-color LED lighting device (CCS; HLV-3M-RGB-3W) and a color camera (Basler; sca640-70gc). The nominal center wavelength of each LED is B(470nm), G(530nm), and R(627nm). Figure 3 shows the spectral sensitivity characteristics of the color camera and the center wavelengths of the three LEDs. By decomposing the color image captured by a color camera and three LEDs illumination, three interference images corresponding to each wavelength can be obtained.

### 2.2 Crosstalk correction

Since the spectral sensitivity curves of the cameras overlap as shown in Fig. 3, there is crosstalk in the B, G, and R signals. Therefore, crosstalk correction is performed assuming that the observed brightness *(B',G',R')* is expressed by the true brightness (*B,G,R*) and the crosstalk coefficients $k_{GB}$, $k_{RB}$, $k_{BG}$, $k_{RG}$, $k_{BR}$, $k_{GR}$; [20)]

$$\begin{pmatrix} B' \\ G' \\ R' \end{pmatrix} = \begin{pmatrix} 1 & k_{GB} & k_{RB} \\ k_{BG} & 1 & k_{RG} \\ k_{BR} & k_{GR} & 1 \end{pmatrix} \begin{pmatrix} B \\ G \\ R \end{pmatrix} \tag{1}$$

The crosstalk coefficients can be calculated from the correlation of R, G, and B brightness with each lighting turned on individually.

### 2.3 Frequency estimation method

In order to obtain the carrier fringe frequency from the fringe image at high speed and with high accuracy, the method (phase gradient method) developed by the authors is used. [21)]

In this method, a new frequency estimate $\hat{f}$ is obtained by

$$\hat{f} = f' + \frac{1}{2\pi}\left(\frac{d\phi'(x)}{dx}\right) \tag{2}$$

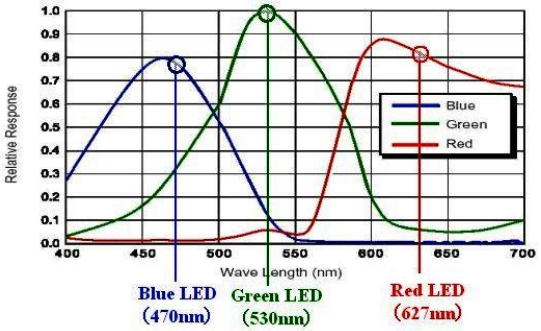


**Fig.3** Spectral response curves of color camera, with the peak wavelengths of three LEDs

where $f'$ is the frequency estimate and $d\phi'(x)/dx$ is the gradient of the estimated phase $\phi'(x)$ which is obtained by least-squares fitting between the observed signal and its sine wave model $g'(x) = A'\cos(2\pi f' x + \phi'(x))$.

The estimation accuracy can be improved by repeating this estimation. For the phase calculation, the local model fitting method described in the next section is used.

### 2.4 Phase calculation method

The phase at each point is found by the local model fitting method (hereinafter referred to as the LMF method)[6)7)]. That is, the brightness data of $n$ points ($n$>=3) near each point are fitted to the sinusoidal model function of the following equation by least squares.

$$g(x,y) = a + b\cos(\phi + 2\pi f_x x + 2\pi f_y y) \tag{3}$$

Here, the three unknown variables are the bias component $a$, the amplitude $b$, and the phase $\phi$, and the carrier fringe frequencies $f_x$ and $f_y$ are obtained in advance by the estimation method in the previous section.

Although this least-squares problem is nonlinear, it can be transformed into a linear least-squares problem by the variable transformations $\xi_c = b\cos\phi$, $\xi_s = b\sin\phi$. Therefore, the unknown variables $a$, $\xi_c$, $\xi_s$ can be obtained analytically by solving the simultaneous linear equations with three unknowns. Phase $\phi$ is calculated by

$$\phi = \operatorname{atan}\left(\frac{\xi_s}{\xi_c}\right) \tag{4}$$

### 2.5 Three-wavelength phase unwrapping

We adopted a method of calculating height candidates from the phases obtained at each wavelength and selecting the best matching height candidate within the expected height range. This method is the

†1 In two-wavelength interferometry, the method of introducing the concept of equivalent wavelength and using 1/2 of that as the measurement range is well known. However, it is shown that this method does not give an accurate measurement range because it does not consider the error and does not effectively utilize the phase information. [17)]

†2 This paper is based on the contents reported in Refs. [17), 18), 19)] and adds the experimental results for an 8 μm step height.

same as the "exact fraction method" [13] that has been used for calibration of block gauges for a long time. Details are given in the next section.

### 2.6 Actual sample measurement experiment

In order to verify the proposed method, we conducted a measurement experiment on a standard step sample with a step difference of about 1130 nm. The experimental device was the Toray Engineering Co., Ltd. surface profiler SP-500 [22] with the illumination/imaging system replaced with a three-wavelength imaging system.

Figure 4 shows the color image obtained by introducing carrier fringes in the horizontal direction. The image data consists of horizontal 512 pixels × vertical 480 pixels × 8 bits × 3 colors. The rectangular discontinuity at the bottom center of the image is the step of about 1 μm. Figure 5 shows the phase profiles of each wavelength obtained by using the LMF method after performing crosstalk correction and frequency estimation from the intensity data of the y=360 line indicated by the white line in Fig. 4. The height profile of the y=360 line calculated from these phase data using the coincidence method is shown by the solid line in Fig. 6. The step height exceeding 1 μm was measured without an error in the order estimation. The dotted line is the coincidence error defined by Eq. (6), which is less than 10 nm except for the step edge. This data is used in Section 4.1. Fig. 7 shows the results of three-dimensional height measurement of the entire surface. It can be seen that the order is correctly estimated over the entire surface except for the edges.

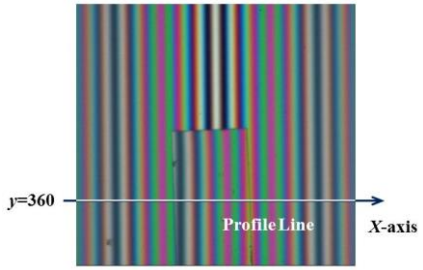


**Fig.4** Color image of 1μm step height (512×480pixel)

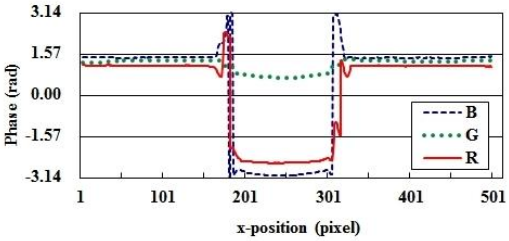


**Fig.5** Phase profiles of three wavelengths at $y$= 360

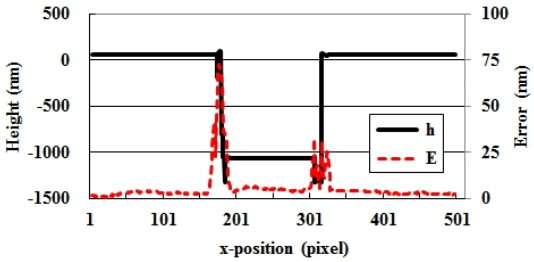


**Fig.6** Height profile at $y$ = 360. The dotted line shows the coincidence error that is referred to later in section 4.1.

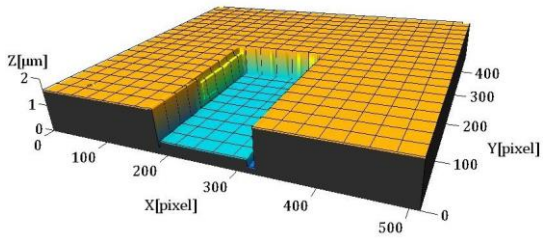


**Fig.7** Measurement result of 1μm step height

## 3. Measurement range estimation method

In this section, after describing the details of the coincidence method algorithm, we discuss how the measurement range is determined, and then derive the estimation method.

### 3.1 Coincidence algorithm

The coincidence method is known as a method for determining height from multiple phase information in multi-wavelength interferometry. For example, in the case of three wavelengths with the wavelength number $i$ ( = 1, 2, 3), the height candidates of each wavelength are obtained from the wavelength $\lambda_i$ and the phase $\phi_i$ by the following equation:

$$h_i(n_i) = \left( \frac{\phi_i}{2\pi} + n_i \right) \left( \frac{\lambda_i}{2} \right), \tag{5}$$

where $n_i$ is the unknown interference order (integer). If there is no error in the phase and the wavelength, the height candidate values of the three wavelengths match at the true height. However, since there is usually an error, as shown in Fig. 8, the combination of height candidate values with the minimum coincidence error (Minimum Error point in the figure) is searched within the expected height range, and let it be the estimated height. As the index of coincidence error, we can use the range (difference between maximum and minimum values), the mean deviation, or variance. From the results of the comparative experiments, it was judged that there is no significant difference between them. Therefore, the range expressed by the following equation was used as the index of the coincidence error.

$$\begin{aligned} E(n_1, n_2, n_3) = & \max[\, h_1(n_1), h_2(n_2), h_3(n_3) \,] \\ & - \min[\, h_1(n_1), h_2(n_2), h_3(n_3) \,], \end{aligned} \tag{6}$$

where max[ ] and min[ ] mean the maximum and the minimum values, respectively.

The specific procedure adopted by the author is described below. Within the given height measurement range, while changing the order $n_3$ of the third wavelength, the height candidate value $h_3(n_3)$ of the third wavelength is calculated by Eq. (5). Next, the height candidate values $h_1(n_1)$ and $h_2(n_2)$ of the first and second wavelengths closest to it are obtained by the following equation.

$$h_i(n_i) = \left( \frac{\phi_i}{2\pi} + \mathrm{Round}\left[ \frac{h_3(n_3)}{(\frac{\lambda_i}{2})} \right] \right) (\frac{\lambda_i}{2}), \qquad (7)$$

where $i$ = 1, 2, and Round[ ] means nearest integer function.

From the obtained combinations of height candidate values, we find the combination that minimizes the coincidence error $E$ expressed by Eq. (6).

Moreover, as the final height calculation formula, a simple average of three candidate height values, a weighted average, etc. can be considered, but the author adopted the simple average expressed by the following formula.

$$h = \frac{h_1(n_1) + h_2(n_2) + h_3(n_3)}{3} \qquad (8)$$

### 3.2 Measuring range in coincidence method

Consider a height range (hereinafter referred to as UMR; Unambiguous Measurement Range) that can be unwrapped without error by the coincidence method. If there is an error in the phase estimation, an error will occur in the height candidate values, and as shown in Fig. 8, the height of the minimum coincidence error may become the height of Next Minimum Error point instead of the Minimum Error point. In this case, the UMR is the interval between them.

Next, let us consider how this UMR is determined. If we assume that the true height is zero †3, all three phases are zeroes. By using Eq. (5), while changing the order $n_3$ of the third wavelength †4, the height candidate $h_3(n_3)$ of the third wavelength and the height candidates $h_1(n_1)$, $h_2(n_2)$ of the first and second wavelengths nearest to it are calculated. Then the coincidence error $E$ is calculated by Eq. (6). In the case of the three wavelengths (B: 470 nm, G: 530 nm, R: 627 nm) used in the three-wavelength single-shot method in the previous chapter, plotting the candidate heights and the coincidence error $E$ gives Fig.9, where the horizontal axis is the height of the third wavelength and the vertical axis is the heights of the nearest neighbor of the first and second wavelengths. This graph is named the Coincidence error diagram.

In this error diagram where the height range is 0 to 5000 nm, the second minimum point of the coincidence error (Next Minimum Error point) is point A, where the height candidate values of each wavelength are 1855, 1880, 1881 nm, the coincidence error is 26 nm, and the average is 1872 nm. The UMR changes depending on whether the phase error in height converted value †5 exceeds 1/2 (13 nm) of the coincidence error (26 nm) at this point. That is, when the phase error is less than 13 nm, the UMR becomes 5000 nm or more, and when it exceeds 13 nm, the height of point A (1872 nm) becomes the UMR.

In the error diagram, the critical points that determine such UMR are the minimum points shown as A, B, C in Fig. 10, and the dotted line connecting these points shows the relationship between the phase error and the UMR. Therefore, if we rewrite the figure and set the horizontal axis to the allowable phase error (1/2 of the matching error) and the vertical axis to the UMR, Fig. 11 is obtained. Using this figure (called UMR diagram), the UMR can be obtained from the phase error. That is, the UMR is 5000 nm or more at 13 nm or less, 1872 nm at 13 to 38.75 nm, 1601 nm at 38.75 to 39 nm, and 271 nm at 39 nm or more.

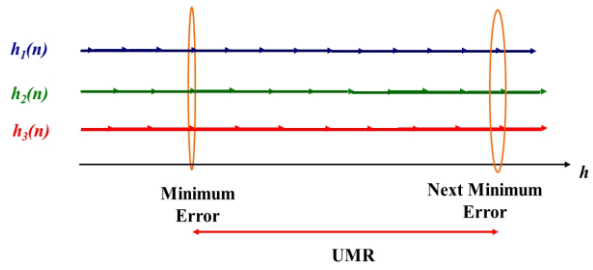


**Fig.8** Exact fraction method and the UMR

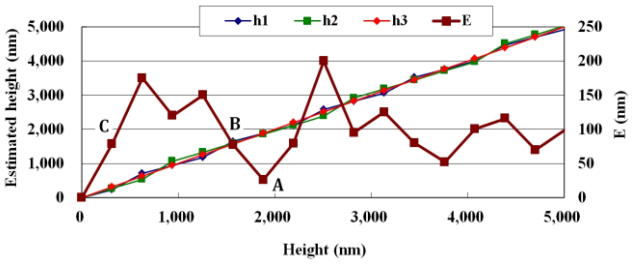


**Fig.9** Coincidence error diagram (470-530-627nm)

†3 The true height was assumed to be 0 to simplify the following discussion, but the graph with the same shape can be obtained at any height with a shifted horizontal axis.

†4 If other wavelength is used as the base wavelength, a slightly different error diagram is obtained. However, since the height candidates of three wavelengths are close to each other near the coincidence point, the selection of the base wavelength does not affect the discussion of the coincidence period. Therefore, the data with the longest wavelength was used in consideration of the calculation load.

†5 Although the coincidence error defined by Eq. (6) includes the phase estimation error and the wavelength error, it will be called as phase error, and expressed in a height converted value.

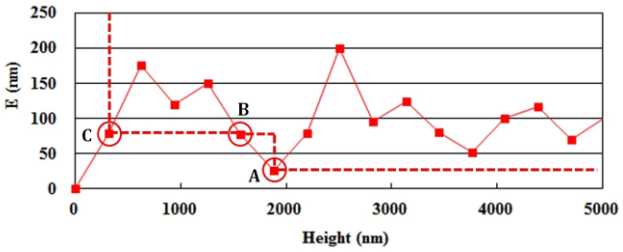


**Fig.10** Coincidence error diagram and its critical points determining the UMR

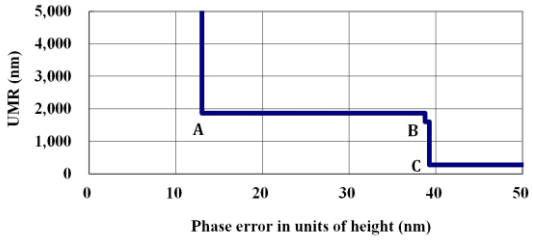


**Fig.11** UMR diagram

### 3.3 Method of estimating measurement range

From the results of the study in the previous section, the measurement range depends on the phase error and can be estimated from the error diagram or UMR diagram. Here, we summarize the range estimation method for three wavelengths.

(1) Create error diagram

(a) Calculate the height candidate value of the third wavelength when the phase is zero by the following formula. The range of order $n_3$ （$n_3$=0,1,⋯） to be calculated is determined from the target height range.

$$h_3(n_3) = (\frac{\lambda_3}{2})n_3 \qquad (9)$$

(b) The height candidate value $h_i$ of the $i$-th wavelength ($i$ = 1, 2) closest to each height candidate value obtained above is calculated by the following equation.

$$h_i(n_i) = \mathrm{Round}\left[\frac{h_3(n_3)}{(\frac{\lambda_i}{2})}\right](\frac{\lambda_i}{2}) \qquad (10)$$

(c) The coincidence error $E$ of the obtained height candidate values is calculated by Eq. (6).

(d) Create an error diagram with $h_3$ on the horizontal axis and $E$ on the vertical axis.

(2) Create a UMR diagram from the minimum point data of the above error diagram.

(3) Obtain the UMR from the expected phase error and set it as the measurement range.

## 4. Wavelength optimization experiment

### 4.1 Optimum wavelength search

Using the range estimation method in the previous section, we obtained the measurement range for various wavelength combinations and searched for the combination that maximizes it (i.e. the optimal wavelengths). The maximum phase error was assumed to be about 10 nm because the coincidence error was less than 10 nm except for the step edge area when a 1 μm step was measured (see Fig. 6).†6 The search range of each wavelength was set to (B) 460 to 480, (G) 500 to 570, and (R) 580 to 630, based on the RGB band of a commercial color camera (see Figs. 3 and 15) and the spectral characteristics of the microscope. Considering the commercially available filters and the accuracy of the center wavelength of the filters, the search pitch was set to 10 nm. As a result, 3 × 8 × 6 = 144 combinations were searched as candidates.

As a search result, the combination of 470 nm (B)-560 nm (G) -600 nm(R) was selected as the optimum wavelength. In this paper, as an example of the search, the error diagram when the first wavelength is fixed at 470 nm, the third wavelength at 600 nm, and the second wavelength at 530, 540, 550, and 560 nm is shown in Fig. 12(a)(b)(c)(d). The UMR diagram is shown in Fig. 13. With the selected 470 nm (B)-560 nm (G) -600 nm (R), the measurement range is expected to be 8.7μm when the phase error is 10 to 15 nm, and 10 μm or more when it is less than 10 nm.

### 4.2 Experiment with the optimum wavelength

4.2.1 Experimental method

In order to confirm the expanded range, a measurement experiment was conducted on a standard step sample with a nominal step of 8 μm.

(1) Interference optics and imaging system

The experimental setup is basically the same as that described in Section 2.6, but the three-wavelength illumination system has a white light source and a multi-bandpass filter (MBPF) as shown in Fig. 14(a) [20]. As shown in Fig. 14(b), this filter has the property of band-passing the three wavelengths selected in the previous section. The bandwidth is 10 nm and the coherence length is about 20μm. The imaging system used a 1.4-megapixel (1360 x 1024 pixel) 3-plate color camera (Hitachi Kokusai Electric, HV-F22CL). Figure 15 shows the spectral sensitivity characteristics of the color camera and the three wavelengths used.

†6） The phase error depends on many factors such as the wavelength error of the illumination light, the aberration of the optical system, the unevenness of the sample surface, vibration, electronic noise, and the phase calculation algorithm. Here, the phase error is estimated from past experimental data (Fig. 6) in which the measurement environment and the sample are similar.

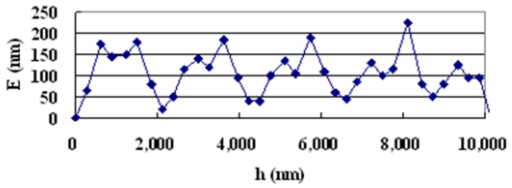


(a) $\lambda_2$ = 530nm

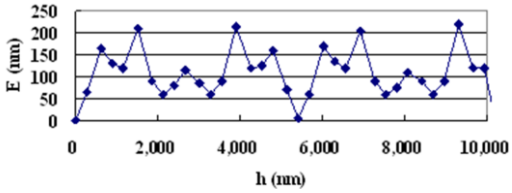


(b) $\lambda_2$ = 540nm

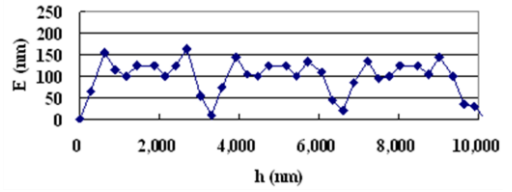


(c) $\lambda_2$ = 550nm

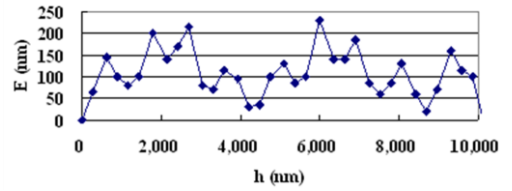


(d) $\lambda_2$ = 560nm

**Fig.12** Coincidence error diagrams to select the optimum second wavelength with the 1st and 3rd wavelengths fixed

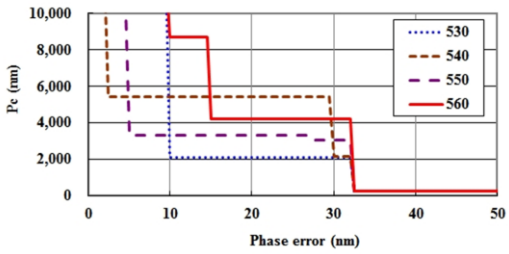


**Fig.13** UMR diagrams of various second wavelengths

(2) Crosstalk compensation

The crosstalk coefficient defined by Eq. (1) was obtained by the method reported by the author. [20] The result is shown below, and the crosstalk is very small. This is in agreement with the prediction from Fig. 15.

$$\begin{pmatrix} B' \\ G' \\ R' \end{pmatrix} = \begin{pmatrix} 1 & 0.00 & 0.00 \\ 0.00 & 1 & 0.00 \\ 0.00 & 0.11 & 1 \end{pmatrix} \begin{pmatrix} B \\ G \\ R \end{pmatrix} \quad (11)$$

Using this coefficient, crosstalk correction was performed, that is, the true brightness (B, G, R) was found from the observed brightness (B', G', R').

4.2.2 Experimental results

In order to facilitate comparison with the conventional method, the central 512 × 480 pixel area of the image captured by the high-resolution camera was used as the measurement target. The color image is shown in Fig. 16, and the three wavelength phases at the

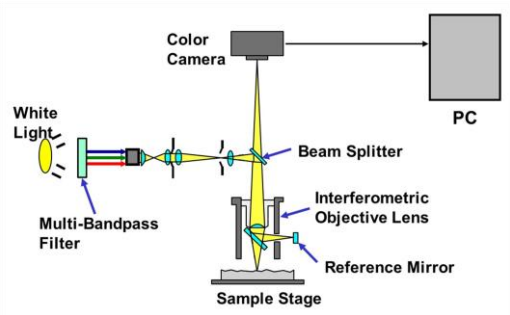


(a) Optical configuration

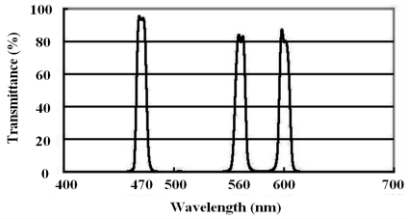


(b) Spectral transmittance of Multi-Bandpass Filter

**Fig.14** Experimental setup

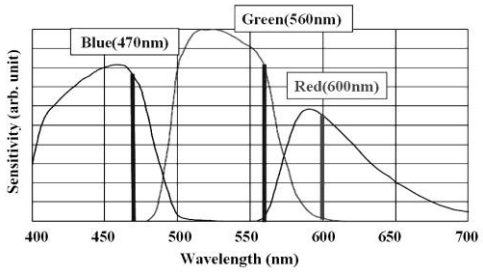


**Fig.15** Spectral sensitivity of camera and three wavelengths

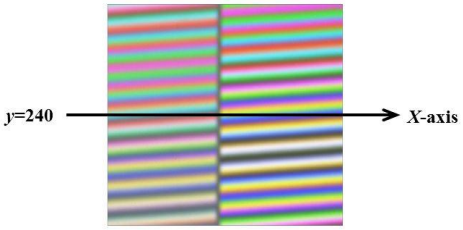


**Fig.16** Color image of 8 micron step height

y=240 line are shown in Fig. 17. The data size used by the LMF method is 5 pixels horizontally × 25 pixels vertically. Furthermore, the profiles of the height and the coincidence error are shown in Fig.18. The coincidence error was 10 nm or less except for the edge areas. This satisfies the condition of 15 nm or less, which is required to achieve the range of 8μm. Figure 19 shows the measurement results for the entire area. A step of 8μm could be measured stably, and the measurement reproducibility (σ) was about 1 nm. The calculation time of the area was about 200 ms on a Windows PC (CPU: Intel Core i7 2.5 GHz).

## 5. Conclusion

In order to expand the measurement range of three-wavelength single-shot interferometry, we made an analysis of the coincidence method in phase unwrapping, and found a new method that can estimate the measurement range for any combination of wavelengths with the phase error given. This made it possible to search for the optimum combination of wavelengths. The optimum wavelength was searched for on the premise of using a commercial color camera, and the wavelength combination of 470 nm (B)-560 nm(G) -600 nm(R) was selected. Using this wavelength combination, it was experimentally confirmed that the surface profile of a standard step sample of 8 μm can be measured stably.

The proposed method can be applied to other multi-wavelength interferometry such as multi-wavelength phase shifting interferometry.

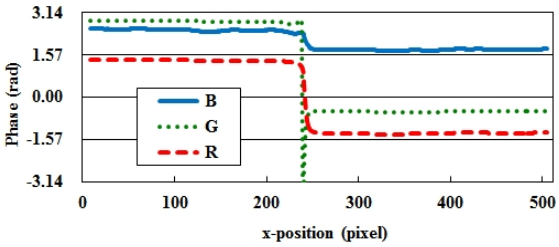


**Fig.17** Phase profiles of three wavelengths at *y*=240

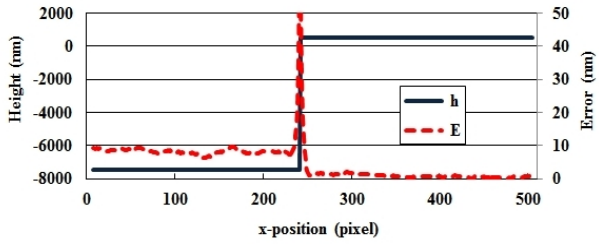


**Fig.18** Height and coincidence error profiles at *y*=240

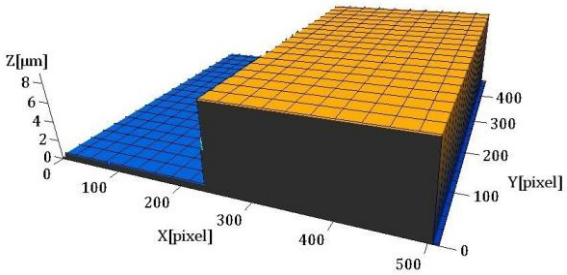


**Fig.19** Measurement result of 8μm step height

## References


1) J. Kato: Real-time fringe analysis for interferometry and its applications, J. Jpn. Soc. Precis. Eng., **64**-9, 1289/1293 (1998) (in Japanese).

2) M. Takeda, H. Ina and S. Kobayashi: Fourier-transform method of fringe-pattern analysis for computer-based topography and interferometry, J. Opt. Soc. Am., **72**-1, 156/160 (1982)

3) S. Toyooka and M. Tominaga: Spatial fringe scanning for optical phase measurement, Opt. Commun., **51**-2, 68/70 (1984)

4) K. H. Womack: Interferometric phase measurement using spatial synchronous detection, Opt. Eng., **23**-4, 391/395 (1984)

5) J. Kato, I. Yamaguchi, T. Nakamura and S. Kuwashima: Video-rate fringe analyzer based on phase-shifting electronic moire patterns, Appl. Opt., **36**-32, 8403/8412 (1997)

6) M. Sugiyama, H. Ogawa, K. Kitagawa and K. Suzuki: Single-shot surface profiling by local model fitting, Appl. Opt., **45**-31, 7999/8005 (2006)

7) M. Sugiyama, T. Matsuzaka, H. Ogawa, K. Kitagawa and K. Suzuki: One-shot profiling of sharp bumpy surfaces, Proc. of JSPE Spring Meeting, 585/586 (2007) (in Japanese).

8) K. Kitagawa, M. Sugiyama, T. Matsuzaka, H. Ogawa and K. Suzuki: Two-wavelength single-shot interferometry, Proc. of SICE Annual Conference 2007, 724/728 (2007)

9) K. Kitagawa, M. Sugiyama, T. Matsuzaka, H. Ogawa and K. Suzuki: Two-Wavelength Single-Shot Interferometry, Proc. of Vision Engineering Workshop (ViEW), 87/92 (2007) (in Japanese).

10) K. Kitagawa: Three-wavelength single-shot interferometry, JSPE Autumn Meeting, 179/180 (2008) (in Japanese).

11) K. Kitagawa: Fast surface profiling by multi-wavelength single-shot interferometry, International Journal of Optomechatronics, **4**-2 136/156 (2010).

12) Y.-Y. Cheng and J.C. Wyant: Two-wavelength phase shifting interferometry, Appl. Opt., **23**-24, 4539/4543 (1984).

13) C. R. Tilford: Analytical procedure for determining lengths from fractional fringes, Appl. Opt. **16**-7, 1857/1860 (1977).

14) A. Pförtner and J. Schwider: Red-green-blue interferometer for the metrology of discontinuous structures, Appl. Opt., **42**-4, 667/673 (2003).

15） C. E. Towers, D. P. Towers and J. D. Jones: Generalized multifrequency selection for full-field interferometric shape measurement, Proc. SPIE **5502**, 406/409 (2004).

16） K. Falaggis, D. P. Towers and C. E. Towers: Optimum wavelength selection for the method of excess fractions, Proc. SPIE **7063**, 70630V/70630V-9 (2008).

17） K. Kitagawa: Study on industrial surface profile measurement method based on optical interferometry, 102-119, Doctoral Dissertation, University of Tokyo (2011) (in Japanese).

18） K. Kitagawa, T. Tsuboi, K. Suzuki and M. Otsuki: Automatic film thickness measurement system of inkjet-based color filters by Three-Wavelength Single-Shot Interferometry, 2010 JSPE Spring Meeting, 881/882 (2010) (in Japanese).

19） K. Kitagawa, H. Sugihara, T. Tsuboi, K. Suzuki and M. Otsuki: Automatic film thickness measurement system for inkjet-based color filters based on three-wavelength single-shot interferometry, J. Jpn. Soc. Precis. Eng., **78**-1, 86/91 (2012).

20） K. Kitagawa: Crosstalk compensation for three-wavelength interferometry, SICE Trans. on Industrial Application, **8**-14, 113/116 (2009) (in Japanese).

21） K. Kitagawa: Two-dimensional frequency estimation for fringe analysis by phase gradient detection, SICE Trans. on Industrial Application, **8**-13, 108/112 (2009) (in Japanese).

22） Toray Engineering Co. 3-D Non-Contact Surface Profiler SP-700/500 Series. http://www.toray-eng.com/lcd/inspection/lineup/sp-500.html (accessed 2013.5.8)

## [About the author]

**Katsuichi Kitagawa (regular member)**

Graduated from the Department of Engineering, University of Tokyo in 1964. In the same year, joined Toray Industries, Inc. Since 1989, engaged in R&D of semiconductor inspection equipment based on the image processing technology. Since 2000, worked at Toray Industries, Inc. Received the 2001 Technology Award of SICE (the Society of Instrument and Control Engineers), the ViEW2003 Odawara Award, the Tejima Memorial Foundation Invention Award, the 2011 Technology Award of JSPE (the Japan Society for Precision Engineering), the 2012 Best Paper Award of JSPE. Advanced Measurement and Control Engineer (authorized by SICE). Ph.D. of Information Science and Engineering (2011, University of Tokyo).

This is an English translation of the paper:
Katsuichi Kitagawa: "Optimum Wavelength Selection to Extend the Unambiguous Measurement Range of the Three-wavelength Single-shot Interferometry", Transactions of SICE, 50(4), 335-341 (2014) (in Japanese).
[translated by the author]